Journal of Molecular Liquids 320 (2020) 114470

Contents lists available at ScienceDirect

Journal of Molecular Liquids

journal homepage: www.elsevier.com/locate/molliq

Magnetic hyperthermia study of magnetosome chain systems in tissue-mimicking phantom

M. Molcan [a,*], K. Kaczmarek [b], M. Kubovcikova [a], H. Gojzewski [c,d], J. Kovac [a], M. Timko [a], A. Józefczak [b]

[a] Institute of Experimental Physics, Slovak Academy of Sciences, Watsonova 47, Košice 040 01, Slovakia
[b] Institute of Acoustics, Faculty of Physics, Adam Mickiewicz University, 61-614 Poznań, Poland
[c] Poznan University of Technology, Faculty of Materials Engineering and Technical Physics, Piotrowo 3, 60-965 Poznań, Poland
[d] University of Twente, Materials Science and Technology of Polymers, Faculty of Science and Technology, Drienerlolaan 5, 7522 NB Enschede, the Netherlands

ARTICLE INFO

Article history:
Received 27 July 2020
Received in revised form 24 September 2020
Accepted 28 September 2020
Available online 2 October 2020

Keywords:
Magnetosomes
Magnetic hyperthermia
Tissue-mimicking phantom
Specific absorption rate
Magnetic relaxation

ABSTRACT

Magnetosomes produced by magnetotactic bacteria are biological membrane-enveloped magnetic nanoparticles. Extracted magnetosomes having the form of long chains as well as shortened chains with individual magnetosomes were prepared. The morphology (chain sizes) was modified in the sonication process and its impact was studied by transmission electron microscopy and dynamic light scattering. Fast magnetization saturation of magnetosome samples and the Verwey transition were detected by temperature-dependent magnetization measurements. To study the heating response to the applied alternating magnetic field (magnetic hyperthermia) magnetosomes were added into tissue-mimicking phantom. Temperature evolution and specific absorption rate (SAR) were measured and analyzed. It was found that embedding magnetosome chains in gel phantoms lead to a noticeable decrease in the efficiency of heating due to deterioration of Brownian mechanism.

1. Introduction

An interesting way to obtain magnetic nanoparticles suitable for bio/tech-purposes is to synthesize particles by a biomineralization process in magnetotactic bacteria (MTB). Magnetotactic bacteria are a group of unique aquatic prokaryotes that contain a chain of intracellular magnetic crystals called magnetosomes. Magnetic properties of magnetosomes inside bacteria are needed to ensure their navigation. They serve as a compass that helps bacteria to orient themselves in sediment and seek food. This ability is called magnetotaxis [1]. The magnetosome chains consist of two phases – the mineral phase of individual ferrimagnetic iron oxide crystals – magnetite (Fe_3O_4), or iron sulfide – greigite (Fe_3S_4) and the organic phase – biological membrane. The membrane is composed of a phospholipid bilayer that encapsulates individual magnetosome crystals as well as many specific proteins. One of the most important is *Mms6* – an acidic protein that provides iron-binding activity from the environment, allowing uniform magnetic crystals forming by precipitating ferrous and ferric ions. The important role of the biological membrane is, among others, to prevent the coagulation of the particles and to ensure the rapid binding of bioactive substances after isolation of the magnetosomes from the bacterium [2].

The size of the biogenic magnetosome crystals, regardless of whether they consist of magnetite or greigite, depends on the MTB species and generally ranges from 35 to 120 nm. In this range, the magnetite crystals have the character of single-domain particles. It indicates that each crystal is a small permanent magnet [3–5]. Considering the high crystalline structure, nanoscale narrow size distribution, biological membrane, magnetic and eco-friendly properties [6] magnetosomes found various applications in nanomedicine. Biocompatible coated magnetosomes have already been used for immobilization, molecules separation, immunoassay, drug carriage, gene therapy, magnetic resonance imaging (MRI) as well as magnetic hyperthermia (MH) and thermoablation [3,7–10]. Based on many current scientific studies and the above-mentioned properties, the most promising application area for magnetosomes seems to be MH for cancer treatment.

MH is the artificially induced increase in temperature in the cancer tissue through the heat produced by magnetic particles. The reason for applying this procedure is that the cancerous cells are sensitive to temperature rise. It can easily lead to their death, while the healthy cells are more resistant to the heat-related damage. In general, the heating arises as a result of particle exposure to the alternating magnetic field, where the magnetic energy is converted to heat due to the relaxation (Brownian and/or Neél) and hysteresis processes. Magnetosomes exhibit high specific heating powers in an alternating magnetic field compared to other studied magnetic nanoparticles [11–13]. This enhancement has its origin in the fact that magnetosomes are arranged in the chain and thus possess higher impact on magnetocrystalline and shape anisotropy. The main challenge in the search of new potential agents for MH is to achieve, as high as possible, specific heating power at

* Corresponding author.
E-mail address: molcan@saske.sk (M. Molcan).

https://doi.org/10.1016/j.molliq.2020.114470
0167-7322/

given monitored conditions (magnetic field amplitude, frequency, particles permeability, size, and shape). It is important for reducing the useful dosage applied to the tumor [14]. Except for the sample characteristics and applied experimental conditions (magnetic field intensity (H), frequency (f)) during MH, it is necessary to analyze many other factors such as compressibility of an environment that surrounds nanoparticles.

Most of the MH experiments are performed on colloidal suspensions. However, such conditions cannot simulate *in vivo* applications. In living organisms/human tissues the environment that surrounds particles has completely different characteristics. Therefore, it influences the physical principles ongoing in magnetic nanoparticle during the application of the AC field [15]. In the tissue Brownian motion is partially immobilized/blocked, and accordingly the amount of released heat is changed. For this reason, it is desirable to investigate the heating effect under the most realistic tissue-like conditions. Gel models are inexpensive and suitable for simulating such conditions. The MH of magnetite nanoparticles embedded in the commercial gel, which melts above 30 °C, was studied by Hiergeist et al. [16]. In the case of ferromagnetic samples, considerable power loss was found in liquid sol in comparison to solid gel. In contrast, for a dissolved ferrofluid, only a small temperature rise was observed at the melting point of the gel. This is due to the negligible influence of Brownian losses for such small particles. Therefore, it is of importance to investigate individual magnetosome samples or magnetosomes with fewer particles per one chain. This magnetosome partition can be achieved by the application of mechanical forces in the sonication process. Sonicated magnetosomes were previously studied in [17,18]. The authors calculated contribution of the relaxation and hysteresis processes on the length-modified magnetosomes. The magnetic properties of immobilized in the gel magnetosomes (isolated from bacteria *Magnetospirillum gryphiswaldense*) were previously studied by Hergt et al. [14]. They measured minor hysteresis loops and by integrating them, hysteresis loss per cycle was determined as a dependence on a magnetic field amplitude. For low field intensities a square-law that changes above about 2 kA/m to a third-order power-law, which is typical for the Rayleigh regime [19], was previously found and reported for small particles.

The promising results of magnetosome magnetic hyperthermia have already been reported by various authors [20–23]. Magnetic hyperthermia used for cancer treatment shows less significant side-effects compared to chemotherapy and radiotherapy [24]. Moreover, the excellent specific absorption rates (SAR) values were determined [14,25,26] as well as cytotoxicity assessment were performed [27–29]. As it was mentioned before the most MH experiments were performed on colloidal suspensions. The impact of surrounding media and modelling properties of tissue were not taken into account. In the proposed paper we present experimental results obtained for the magnetosomes extracted from the bacteria *Magnetospirillum* sp. *strain AMB-1* that served for the preparation of the agar-based tissue-mimicking phantoms and liquid suspension. MH measurements were conducted and the obtained results were compared and discussed.

2. Materials and methods

2.1. Preparation of magnetosomes

For our studies magnetite magnetosomes extracted from *Magnetotacticum Spirillum - AMB 1* were used. The bacteria synthesis process and isolation of chain particles were done under our laboratory conditions, thereafter modified to shorten their chains. Details are described in Molcan et al. [18] and Dzarova et al. [30]. The samples differed in chain-length which enabled us to observe the effect of magnetosome sizes on their heating properties. The first sample consisted of original long-isolated chains (IM) dispersed in HEPES buffer. The second sample (SM) was prepared by sonication of IM magnetosome suspension using SonifierCell Disruptor, Branson Ultrasonics, model 450, USA. The mechanical forces transmitted by the micro-tip probe caused the structural changes in IM sample and thus in the size distribution of long chains. The used sonication parameters were as follows: frequency - 20 kHz, ultrasonic wave intensity (estimated using calorimetric method [31]) ~10 W/cm^2, time = 1 h. During sonication, to prevent the thermal denaturation of the membrane or degradation of the sample, the sample was constantly cooled down with ice added to the bath.

2.2. Preparation of tissue-mimicking phantom

Magnetic heating experiments were performed on a magnetosomes suspension and agar-based phantoms. Tissue-mimicking phantoms are widely used in hyperthermia and thermal ablation studies [32–34]. The phantom systems mimicking human tissues have a more realistic performance perspective. Custom made agar-based phantoms, with specific and controlled properties, offer the possibility to conduct experiments in conditions similar to the human body [35]. Agar powder was dissolved in the hot suspension of magnetosome chains and then left to cool down. To prepare 5% (w/w) agar phantoms doped with magnetosome chains, 1.5 ml magnetosome chains suspension was mixed with 0.0789 g of standard plate count agar powder (Plate-Count-Agar according to Buchbinder et al., product no. 88588, Sigma-Aldrich Co.).

2.3. Characterization methods of magnetosome particles

The prepared magnetosome particles were accurately characterized by various methods.

2.3.1. Transmission electron microscopy (TEM)

Sample preparation: using a syringe with a stainless steel needle, a micro-droplet of the magnetosome suspension was put on a carbon-coated copper support grid. Drying was done in the air. TEM analysis was performed in a Philips CM300ST FEG Transmission Electron Microscope at used acceleration voltage 300 kV in a bright field.

2.3.2. Dynamic light scattering (DLS)

The hydrodynamic size distribution of the samples were compared by DLS measurements using the Zetasizer Nano ZS (Malvern Instruments, UK) with a 4 mW He-Ne laser, $\lambda = 633$ nm. The scattering angle was 173° and applied temperature 25 °C. Using this apparatus the zeta potential of the samples was also measured.

2.3.3. Magnetization measurements

Magnetization measurements were carried out by SQUID magnetometer (Quantum Design MPMS 5XL) in the magnetic field up to 100 kA/m. The magnetization curves were measured at room temperature. Temperature-dependent measurements (known as the zero-field cooled (ZFC) and field cooled (FC) magnetization curves) were performed in the range from 2 K up to 250 K. The ZFC-FC measurements were carried out in the presence of the applied field of ~8 kA/m (100 Oe). The measurement process is as follows: a) ZFC magnetization – at the beginning, the sample is cooled from room temperature to 2 K in the absence of the applied magnetic field. Subsequently, the magnetization is measured with increasing the temperature in the presence of the field; b) FC magnetization – the magnetization is measured by cooling the sample in the presence of the magnetic field.

2.4. Calorimetric measurements in magnetic field

During magnetic hyperthermia experiments as a source of the alternating magnetic field (AMF), the compact EASYHEAT (Ambrell Corporation, United States) induction heating system was used. The setup consisted of a high-frequency power supply and the water-cooled induction heating coil. The induction coil had a length of 60 mm and

five turns of 56-mm diameter. The frequency of the alternating magnetic field was 356 kHz and the intensity was ranging from 10.7 to 16.2 kA/m. During measurements research material (magnetosome chains suspension/agar phantom with magnetosome chains) was centrally placed and thermally insulated in a water-cooled magnetic induction coil. The temperature in the materials during magnetic heating experiments was measured using an optic fiber probe (model FTP-NY2) connected to FLUOTEMP temperature sensor system (Photon Control Inc.). During experiments, the optical fiber was centrally placed in the material. The single measurement lasted 180 s. The calibration curve was subtracted from every measurement curve ensuring that the presented in Figs. 6–7 temperature rises are from purely magnetic heating mechanisms. The scheme of the calorimetric measurements setup is presented in Fig. 1.

3. Results and discussion

3.1. Properties of magnetosomes

3.1.1. Size analysis (TEM, DLS)

The impact of sonication on magnetosome chains length is shown in Fig. 2. The image marked as IM represents isolated magnetosomes in the form of long chains that were not influenced by the sonication process. Chains composed of several particles are clearly visible. SM sample is a mixture of single magnetosomes and shortened chains composed of a few particles per one chain. We already studied the magnetosome particles size distribution in the article by Gojzewski et al. [36] and we obtained the following mean size and its standard deviation: 43 ± 12 nm.

The obvious impact of sonication on the size distribution was also confirmed by DLS measurements (Fig. 3). The hydrodynamic size of the magnetosomes decreased from 600 nm in IM sample to 400 nm after sonication. Both samples showed a bimodal size distribution. IM exhibits broader size distribution as the SM.

Both techniques (TEM, DLS) used for size distribution analysis showed the reduction in chains length. It should be noted that these methods are based on different physical principles and thus the obtained numerical values are not comparable. While TEM provides the size of the particle cores, DLS gives hydrodynamic size that includes the layer of liquid medium surrounding the chains.

Additionally, the zeta potential measurements were carried out. Zeta potentials help to characterize the surface of the particles as they can give information about the overall surface charge of the particles (magnetosomes). The measured values of −22 mV (IM) and −15 mV (SM) indicate that the magnetosomes are at the edge of the stability region in the present environment (HEPES buffer) leading to slight aggregation and consequent sedimentation.

3.1.2. Magnetization characteristics

Both IM and SM samples exhibit a similar character of magnetization curves. One can see a fast magnetization saturation (M_S) as it is typical for superparamagnetic nanoparticle systems (although small hysteresis become apparent). In the case of IM sample, the M_S is achieved at ~10kA/m, and in the case of SM sample saturates even sooner. This difference can be ascribed to smaller and narrower size distribution proved by DLS measurements.

Temperature-dependent magnetization measurements known as ZFC-FC curves are presented in Fig. 5. The used magnetic field was sufficient to register the Verwey transition. The Verwey transition is a low-temperature phase transition in the mineral magnetite near 125 K. This transition is observed as a sharp change in the magnetic moment at the transition temperature, which is typical for bulk magnetite material [8,37]. The fact that we can observe this transition in a nano-sized magnetite system demonstrates the good quality of Fe_3O_4 crystallites. In studied magnetosome systems (IM, SM) the temperature of Verwey transition is shifted to 102 K as a result of nano-size character of magnetite.

In order to graphically highlight the temperature of Verwey's transition the ZFC data were plotted as 1st derivative *vs.* temperature, as it is presented in inset of Fig. 5.

3.2. Heating of magnetosome chains

The most important part of this research was the measurement of the heating effect caused by magnetosome chains in an alternating

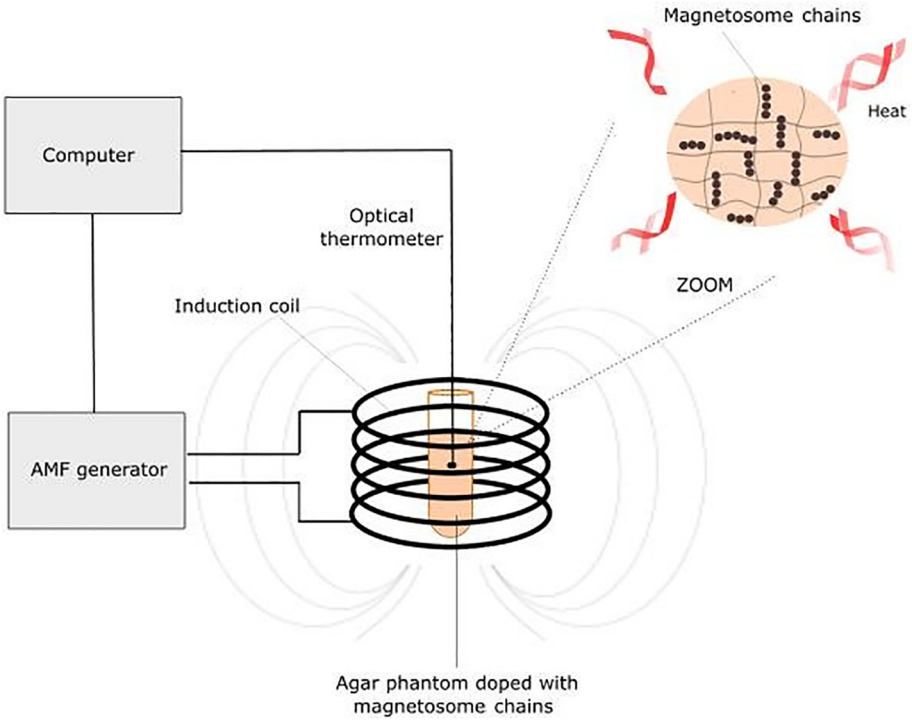

Fig. 1. The scheme of calorimetric measurements setup.

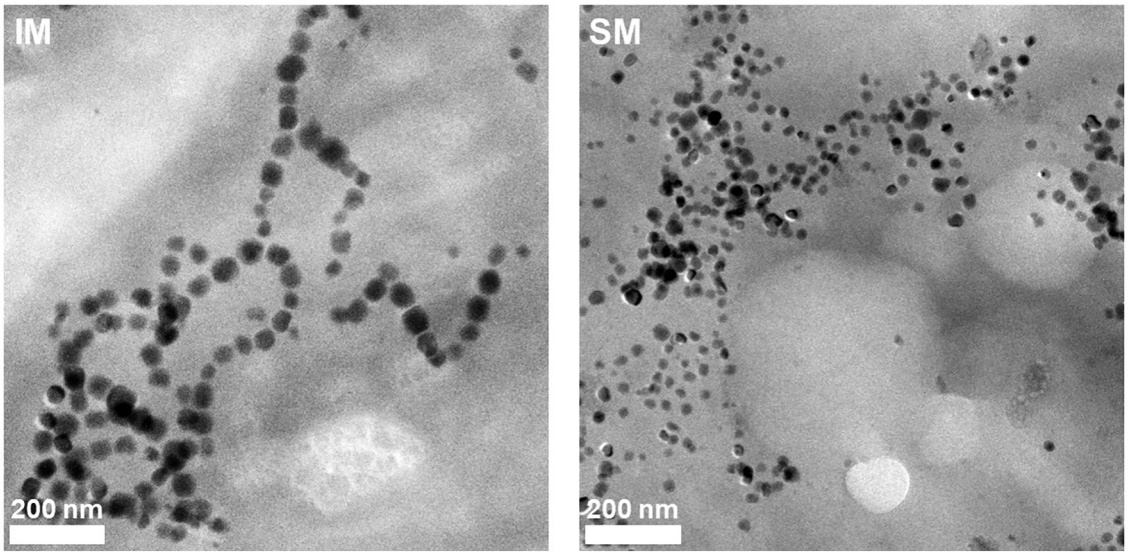

Fig. 2. TEM images of IM and SM magnetosomes.

magnetic field. The temperature increase was carefully measured and registered during the magnetic heating process of magnetosome chains suspension and agar phantom doped with magnetosome chains.

Fig. 6 compares the results of magnetic hyperthermia for IM magnetosomes suspensions and agar phantoms doped with IM magnetosomes. For 16.2 kA/m there is a significant difference between temperature rise for suspension and agar phantom. In magnetosomes suspension temperature increases about 3.8 °C however for agar phantom about 2.2 °C. This noticeable temperature drop results from partial blockage of the Brownian mechanism caused by the confinement of magnetosomes chains in the gel-structure of agar phantom. Tissue-mimicking phantom doped with magnetosomes has a higher bulk modulus K (smaller compressibility characterized as $\beta_s = 1 / K$) than magnetosomes suspension [19]. The Brownian effect in materials with smaller compressibility, such as gels or tissues, is very limited due to the fairly fixed position the particles or particle chains occupy in the medium. In suspension, nanoparticles move freely and generate heat easily. However, lack of noticeable difference between temperature rises for suspension and agar phantom for 13.5 kA/m indicates that only Néel relaxation mechanism was present. It can be assumed that 10.7 and 13.5 kA/m of AMF provided insufficient energy to activate the Brownian mechanism and rotate magnetosomes. Therefore, observed temperature rise was only from the Néel relaxation. More energy needs to be provided to activate both thermal mechanism in magnetic hyperthermia (Néel and Brownian).

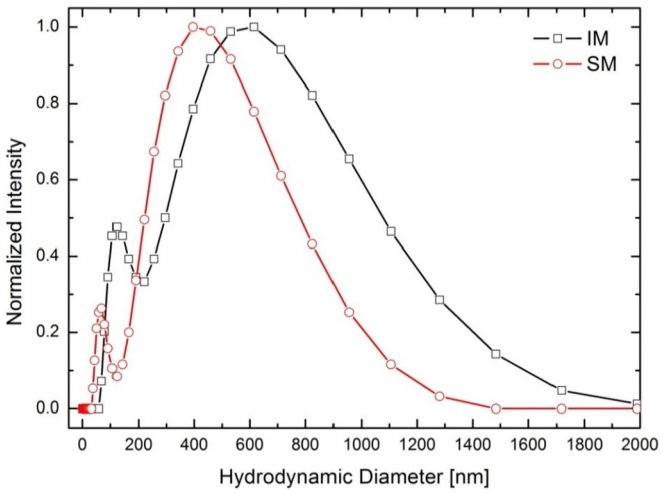

Fig. 3. Normalized distribution of hydrodynamic diameter of IM and SM magnetosomes.

Fig. 7 compares the results of magnetic hyperthermia obtained for SM suspensions and agar phantoms doped with SM. For each magnetic field intensity, there is a visible difference between temperature rise obtained for suspension of SM and agar phantom doped with SM. In magnetosome chains suspension, temperature increases were always higher comparing to those observed for phantoms. This temperature drop once again can be explained by partial blockage of the Brownian mechanism caused by the confinement of magnetosomes in the gel-structure of agar phantom. Comparing hyperthermia results for SM (Fig. 7) to IM (Fig. 6) suspension it can be seen that SM provides better heating results. Process of sonication raptures magnetosome chains leading to their shortening or overall disintegration to single nanoparticles. It affects the properties of magnetosomes as a heat nano-source. Raptured chains or single nanoparticles (SM), due to their smaller overall size, have a better chance not to be confined by gel structure and in consequence better chance to rotate due to the Brownian mechanism, which explains the observed more efficient heating effect.

Figs. 8 and 9 compare specific absorption rate (SAR) values for magnetic hyperthermia in a function of magnetic field intensity for SM/IM suspensions and agar phantoms doped with SM/IM. The specific absorption rate volume was evaluated to characterize the power deposition of thermal treatment. The SAR value depends on the efficiency of the heat source and the ability of the heated medium to absorb thermal energy. Thus, the SAR value depends on the magnetosome concentration and their ability to rotate (Brownian mechanism) in material. According to the definition, the SAR describes the rate of energy absorption by a material, and can be calculated as:

$$SAR = \frac{C_p \rho_S}{m} \left(\frac{dT}{dt}\right) \quad (1)$$

where C_p is the specific heat capacity ($C_p \approx C_{water} = 4.18\,\mathrm{J \cdot K^{-1} \cdot g^{-1}}$), ρ_S is the density of the sample ($\approx 1021\,\mathrm{kg \cdot m^{-3}}$), m is the mass of magnetite per unit volume of the colloid (1.8 mg/ml for SM and 1.6 mg/ml for IM) and dT/dt is the heating rate (slope) calculated from the linear fit to the heating curves. In practice, obtaining the SAR involves fitting the resulting experimental data of temperature to a linear function of time, and then determining its slope at time zero. It can be seen that SM/IM suspensions obtained higher SAR values than phantoms doped with SM/IM. This SAR dependence can be explained by partial blockage of

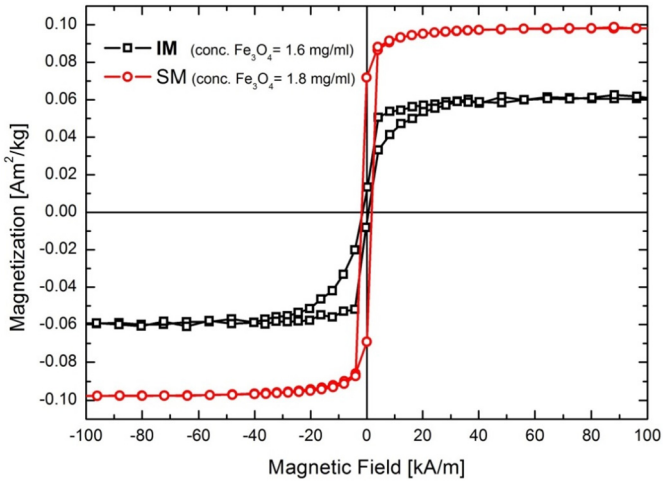

Fig. 4. Magnetization curves of IM and SM magnetosome colloids measured at room temperature (293 K).

the Brownian mechanism caused by confinement of magnetosomes in the gel-structure of agar phantom. The SAR values decrease with decreasing compressibility of materials. SAR dependence on magnetic field intensity is clearly visible. The higher the intensity the higher the SAR value. It was reported that magnetosome chains exhibit greater heating efficiency comparing to single nanoparticles [38,39]. Here we obtained different results. However, higher value of SAR for SM comparing to IM magnetosome chains can be a result of difference in their magnetization. SM magnetosome chains used in our experiments have slightly higher magnetization than IM magnetosome chains (Fig. 4). Fig. 9 confirmed that chains of nanoparticles, due to their bigger than single particles size, have a smaller ability to move in phantom structure, and in consequence exhibit smaller heating effects.

The magnetic heating effect can be improved. Combining magnetic hyperthermia with other heating methods such as photo heating (photo-thermal therapy) [40] or ultrasound heating (sono-magnetic) [41] can lead to a more effective output. Synergistic interaction between two heating mechanisms can improve the thermal effect of magnetic hyperthermia through unblocking Brownian's relaxation. Synergetic temperature increases phantom pores, allowing nanoparticles to move more freely.

Based on the results of size characteristics and temperature evolution experiments it can be concluded that both investigated

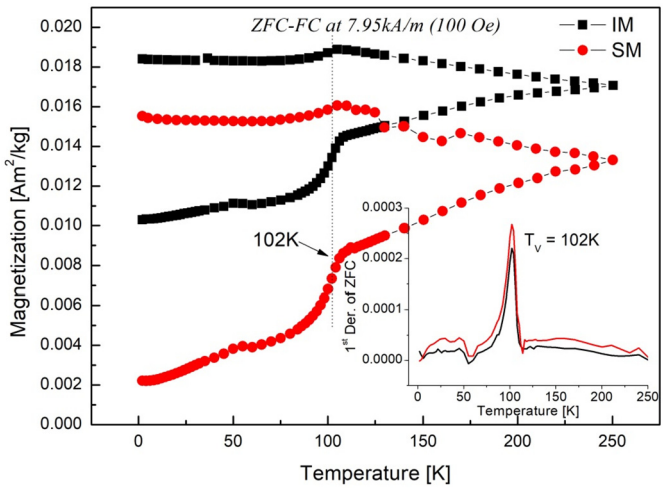

Fig. 5. Zero-field-cooled (ZFC) and field-cooled (FC) magnetization curves as a function of the temperature of IM and SM sample (inset: 1st derivative of ZFC *vs.* temperature).

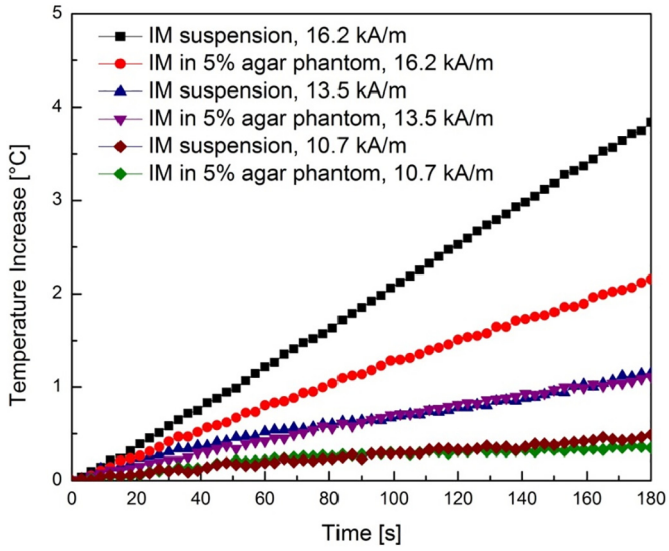

Fig. 6. Magnetic hyperthermia of magnetosome chains suspension and magnetosome chains embedded in agar phantom for different values of AMF (16.2, 13.5 and 10.7 kA/m).

properties – size distribution of samples and environment are important, and should be taken into account during evaluation of MH results. One should note that the Brownian or Néel relaxation is not only dependent on the magnetosomes size, but also on their distribution, which in the case of magnetosomes could be noticeable [36]. We showed that the Brownian mechanism plays important role in heating in liquid media but is suppressed in viscous media (agar gel). In the viscous medium, the main heat contribution comes from the Néel relaxation mechanism.

4. Conclusions

Magnetic hyperthermia is becoming more and more popular. However, most of the magnetic heating experiments are performed in colloidal suspensions, where the conditions cannot simulate *in vivo* applications. It is of importance to remember that in tissues the environment surrounding the particles has significantly different characteristics, which have a significant impact on the effectiveness of magnetic heating. In this work, we performed magnetic heating on magnetosome

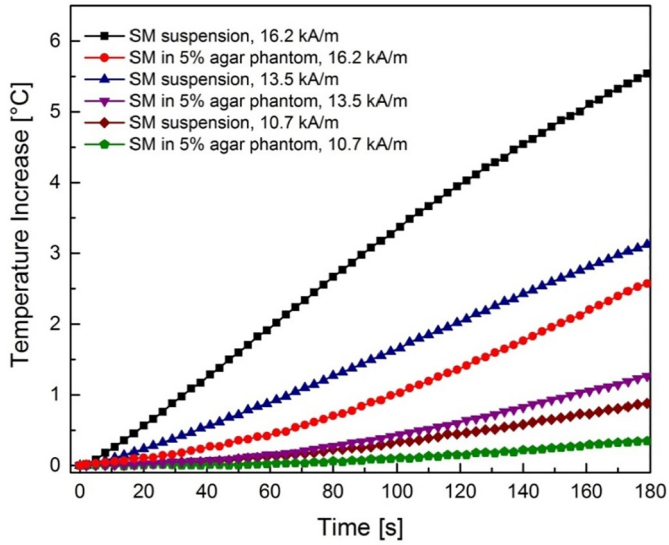

Fig. 7. Magnetic hyperthermia of sonicated magnetosomes suspension and sonicated magnetosomes embedded in agar phantom for different values of AMF.

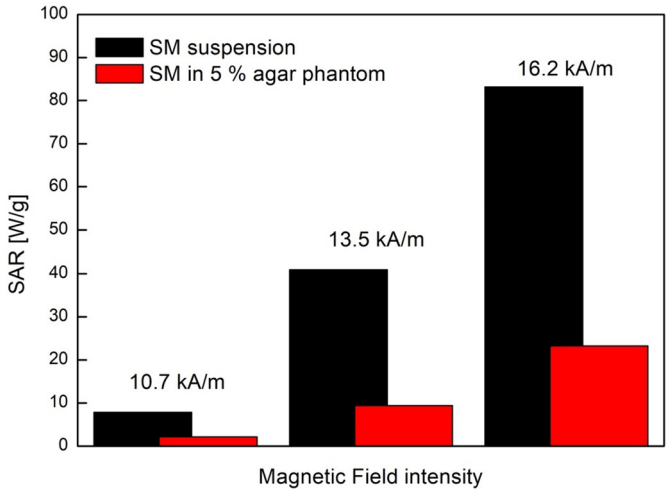

Fig. 8. Specific absorption rate for SM magnetosome suspensions and SM magnetosomes embedded in agar phantom for different values of AMF.

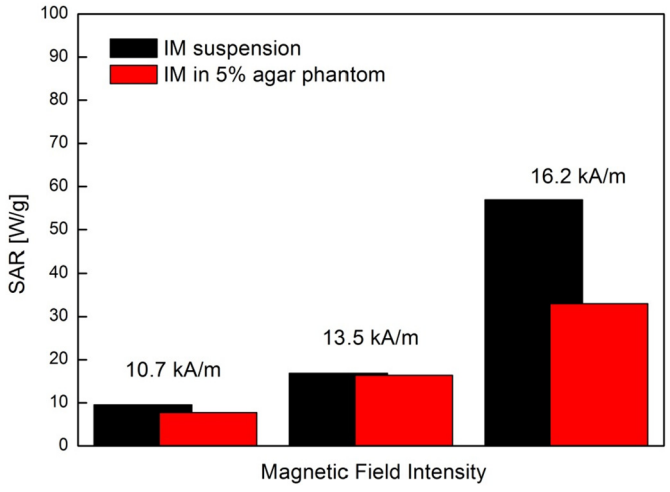

Fig. 9. Specific absorption rate for IM magnetosome suspensions and IM magnetosomes embedded in agar phantom for different values of AMF.

chains suspension and magnetosome chains embedded in tissue-mimicking phantoms. Results show that the environment in which magnetosome chains are embedded affects the temperature increase during magnetic hyperthermia. Placing of magnetosome chains in gel phantoms leads to a noticeable decrease in efficiency of heating due to deterioration of Brownian mechanism.

CRediT authorship contribution statement

Author Contributions: Sample preparation: M.M; Writing – original draft: M.M., A.J., K.K.; Writing – review & editing: M.M., A.J., K.K., H.G., M.K., M.T.; Investigation – M.M., K.K, M.K., H.G., J.K. and A.J.

Declaration of competing interest

The authors declare that they have no known competing financial interests or personal relationships that could have appeared to influence the work reported in this paper.

Acknowledgments

The A. J. and K. K. would like to acknowledge the Polish National Science Centre for support by the grants: 2015/17/B/ST7/03566 (OPUS) and 2017/27/N/ST7/00201 (PRELUDIUM). M. M. and M. T. are supported by the project MVTS M-ERA.NET 2 – FMF, MVTS MAGBBRIS, MODEX (ITMS2014+: 313011T548) and by the Slovak Research and Development Agency under the Contract no. APVV-18-0160, APVV-15-0453. H.G. acknowledges the Ministry of Science and Higher Education for the project no. 06/62/SBAD/1923 realized at the Faculty of Materials Engineering and Technical Physics, Poznan University of Technology, and the support within the Bekker Programme from the Polish National Agency for Academic Exchange.

References

[1] X. Wang, Y. Li, J. Zhao, H. Yao, S. Chu, Z. Song, Z. He, W. Zhang, Magnetotactic bacteria: characteristics and environmental applications, Front. Environ. Sci. Eng. 14 (2020) 1–14, https://doi.org/10.1007/s11783-020-1235-z.
[2] A. Peigneux, Y. Jabalera, M.A.F. Vivas, S. Casares, A.I. Azuaga, C. Jimenez-Lopez, Tuning properties of biomimetic magnetic nanoparticles by combining magnetosome associated proteins, Sci. Rep. 9 (2019) 1–11, https://doi.org/10.1038/s41598-019-45219-7.
[3] L. Yan, S. Zhang, P. Chen, H. Liu, H. Yin, H. Li, Magnetotactic bacteria, magnetosomes and their application, Microbiol. Res. 167 (2012) 507–519, https://doi.org/10.1016/j.micres.2012.04.002.
[4] D. Schüler, Formation of magnetosomes in magnetotactic bacteria, J. Mol. Microbiol. Biotechnol. 1 (1999) 79–86http://www.ncbi.nlm.nih.gov/pubmed/10941788. (Accessed 14 October 2019).
[5] Y. Amemiya, A. Arakaki, S.S. Staniland, T. Tanaka, T. Matsunaga, Controlled formation of magnetite crystal by partial oxidation of ferrous hydroxide in the presence of recombinant magnetotactic bacterial protein Mms6, Biomaterials 28 (2007) 5381–5389, https://doi.org/10.1016/j.biomaterials.2007.07.051.
[6] J. Xu, L. Liu, J. He, S. Ma, S. Li, Z. Wang, T. Xu, W. Jiang, Y. Wen, Y. Li, J. Tian, F. Li, Engineered magnetosomes fused to functional molecule (protein A) provide a highly effective alternative to commercial immunomagnetic beads, J. Nanobiotechnol. 17 (2019) 37, https://doi.org/10.1186/s12951-019-0469-z.
[7] J.J. Jacob, K. Suthindhiran, Magnetotactic bacteria and magnetosomes – scope and challenges, Mater. Sci. Eng. C. 68 (2016) 919–928, https://doi.org/10.1016/J.MSEC.2016.07.049.
[8] M. Timko, M. Molcan, A. Hashim, A. Skumiel, M. Muller, H. Gojzewski, A. Jozefczak, J. Kovac, M. Rajnak, M. Makowski, P. Kopcanský, Hyperthermic effect in suspension of magnetosomes prepared by various methods, IEEE Trans. Magn. 49 (2013)https://doi.org/10.1109/TMAG.2012.2224098.
[9] M. Molcan, V.I. Petrenko, M.V. Avdeev, O.I. Ivankov, V.M. Garamus, A. Skumiel, A. Jozefczak, M. Kubovcikova, P. Kopcansky, M. Timko, Structure characterization of the magnetosome solutions for hyperthermia study, J. Mol. Liq. 235 (2017) 11–16, https://doi.org/10.1016/J.MOLLIQ.2016.12.054.
[10] T. Matsunaga, S. Kamiya, Use of magnetic particles isolated from magnetotactic bacteria for enzyme immobilization, Appl. Microbiol. Biotechnol. 26 (1987) 328–332, https://doi.org/10.1007/BF00256663.
[11] A. Józefczak, B. Leszczyński, A. Skumiel, T. Hornowski, A comparison between acoustic properties and heat effects in biogenic (magnetosomes) and abiotic magnetite nanoparticle suspensions, J. Magn. Magn. Mater. 407 (2016) 92–100, https://doi.org/10.1016/J.JMMM.2016.01.054.
[12] E. Alphandéry, I. Chebbi, F. Guyot, M. Durand-Dubief, Use of bacterial magnetosomes in the magnetic hyperthermia treatment of tumours: a review, Int. J. Hyperth. 29 (2013) 801–809, https://doi.org/10.3109/02656736.2013.821527.
[13] R. Le Fèvre, M. Durand-Dubief, I. Chebbi, C. Mandawala, F. Lagroix, J.-P. Valet, A. Idbaih, C. Adam, J.-Y. Delattre, C. Schmitt, C. Maake, F. Guyot, E. Alphandéry, Enhanced antitumor efficacy of biocompatible magnetosomes for the magnetic hyperthermia treatment of glioblastoma, Theranostics 7 (2017) 4618–4631, https://doi.org/10.7150/thno.18927.
[14] R. Hergt, R. Hiergeist, M. Zeisberger, D. Schüler, U. Heyen, I. Hilger, W.A. Kaiser, Magnetic properties of bacterial magnetosomes as potential diagnostic and therapeutic tools, J. Magn. Magn. Mater. 293 (2005) 80–86, https://doi.org/10.1016/j.jmmm.2005.01.047.
[15] S. Mornet, S. Vasseur, F. Grasset, P. Veverka, G. Goglio, A. Demourgues, J. Portier, E. Pollert, E. Duguet, Magnetic nanoparticle design for medical applications, Prog. Solid State Chem. 34 (2006) 237–247, https://doi.org/10.1016/J.PROGSOLIDSTCHEM.2005.11.010.
[16] R. Hiergeist, W. Andrä, N. Buske, R. Hergt, I. Hilger, U. Richter, W. Kaiser, Application of magnetite ferrofluids for hyperthermia, J. Magn. Magn. Mater. 201 (1999) 420–422, https://doi.org/10.1016/S0304-8853(99)00145-6.
[17] M. Molčan, A. Hashim, J. Kováč, M. Rajňák, P. Kopčanský, M. Makowski, H. Gojzewski, M. Molokác, L. Hvizdák, M. Timko, Characterization of magnetosomes after exposure to the effect of the sonication and ultracentrifugation, Acta Phys. Pol. A 126 (2014)https://doi.org/10.12693/APhysPolA.126.198.
[18] M. Molcan, H. Gojzewski, A. Skumiel, S. Dutz, J. Kovac, M. Kubovcikova, P. Kopcansky, L. Vekas, M. Timko, Energy losses in mechanically modified bacterial magnetosomes, J. Phys. D. Appl. Phys. 49 (2016), 365002, https://doi.org/10.1088/0022-3727/49/36/365002.
[19] S. Chikazumi, C.D. Graham, S. Chikazumi, Physics of Ferromagnetism, Oxford University Press, Oxford; New York, 1997https://www.worldcat.org/title/physics-of-ferromagnetism/oclc/519697464. (Accessed 14 October 2019).
[20] M.E. Fortes Brollo, A. Domínguez-Bajo, A. Tabero, V. Domínguez-Arca, V. Gisbert, G. Prieto, C. Johansson, R. Garcia, A. Villanueva, M.C. Serrano, M.D.P. Morales, Combined

magnetoliposome formation and drug loading in one step for efficient alternating current-magnetic field remote-controlled drug release, ACS Appl. Mater. Interfaces 12 (2020) 4295–4307, https://doi.org/10.1021/acsami.9b20603.
[21] Y. Jabalera, A. Fernández-Vivas, G.R. Iglesias, Á.V. Delgado, C. Jimenez-Lopez, Magnetoliposomes of mixed biomimetic and inorganic magnetic nanoparticles as enhanced hyperthermia agents, Colloids Surf. B Biointerfaces 183 (2019), 110435, https://doi.org/10.1016/j.colsurfb.2019.110435.
[22] G.R. Iglesias, Y. Jabalera, A. Peigneux, B.L. Checa Fernández, Á.V. Delgado, C. Jimenez-Lopez, Enhancement of magnetic hyperthermia by mixing synthetic inorganic and biomimetic magnetic nanoparticles, Pharmaceutics 11 (2019) 273, https://doi.org/10.3390/pharmaceutics11060273.
[23] A. Peigneux, F. Oltolina, D. Colangelo, G.R. Iglesias, A.V. Delgado, M. Prat, C. Jimenez-Lopez, Functionalized biomimetic magnetic nanoparticles as effective nanocarriers for targeted chemotherapy, Part. Part. Syst. Charact. 36 (2019), 1900057, https://doi.org/10.1002/ppsc.201900057.
[24] P. Das, M. Colombo, D. Prosperi, Recent advances in magnetic fluid hyperthermia for cancer therapy, Colloids Surf. B Biointerfaces 174 (2019) 42–55, https://doi.org/10.1016/J.COLSURFB.2018.10.051.
[25] E. Alphandéry, S. Faure, L. Raison, E. Duguet, P.A. Howse, D.A. Bazylinski, Heat production by bacterial magnetosomes exposed to an oscillating magnetic field, J. Phys. Chem. C 115 (2011) 18–22, https://doi.org/10.1021/jp104580t.
[26] R. Hergt, S. Dutz, R. Uller, M. Zeisberger, Magnetic particle hyperthermia: nanoparticle magnetism and materials development for cancer therapy, J. Phys. Condens. Matter. 18 (2006) 2919–2934, https://doi.org/10.1088/0953-8984/18/38/S26.
[27] Z. Varchulova Novakova, I. Gasparova, L. Krajciova, M. Molcan, I. Varga, M. Timko, L. Danisovic, Effect of magnetosomes on cell proliferation, apoptosis induction and expression of Bcl-2 in the human lung cancer cell line A549, Biol 72 (2017)https://doi.org/10.1515/biolog-2017-0059.
[28] L. Qi, X. Lv, T. Zhang, P. Jia, R. Yan, S. Li, R. Zou, Y. Xue, L. Dai, Cytotoxicity and genotoxicity of bacterial magnetosomes against human retinal pigment epithelium cells, Sci. Rep. 6 (2016), 26961, https://doi.org/10.1038/srep26961.
[29] E. Alphandéry, A. Idbaih, C. Adam, J.-Y. Delattre, C. Schmitt, F. Guyot, I. Chebbi, Chains of magnetosomes with controlled endotoxin release and partial tumor occupation induce full destruction of intracranial U87-Luc glioma in mice under the application of an alternating magnetic field, J. Control. Release 262 (2017) 259–272, https://doi.org/10.1016/J.JCONREL.2017.07.020.
[30] A. Dzarova, F. Royer, M. Timko, D. Jamon, P. Kopcansky, J. Kovac, F. Choueikani, H. Gojzewski, J.J. Rousseau, Magneto-optical study of magnetite nanoparticles prepared by chemical and biomineralization process, J. Magn. Magn. Mater. 323 (2011) 1453–1459, https://doi.org/10.1016/J.JMMM.2010.12.041.
[31] T.J. Mason, J.P. Lorimer, D.M. Bates, Quantifying sonochemistry: casting some light on a 'black art, Ultrasonics 30 (1992) 40–42, https://doi.org/10.1016/0041-624X(92)90030-P.
[32] K. Kaczmarek, R. Mrówczyński, T. Hornowski, R. Bielas, A. Józefczak, The effect of tissue-mimicking phantom compressibility on magnetic hyperthermia, Nanomater. (Basel, Switzerland). 9 (2019)https://doi.org/10.3390/nano9050803.
[33] M. Zhang, Z. Che, J. Chen, H. Zhao, L. Yang, Z. Zhong, J. Lu, Experimental determination of thermal conductivity of water—agar gel at different concentrations and temperatures, J. Chem. Eng. Data 56 (2011) 859–864, https://doi.org/10.1021/je100570h.
[34] M. Salloum, R.H. Ma, D. Weeks, L. Zhu, Controlling nanoparticle delivery in magnetic nanoparticle hyperthermia for cancer treatment: experimental study in agarose gel, Int. J. Hyperth. 24 (2008) 337–345, https://doi.org/10.1080/02656730801907937.
[35] K. Manickam, R.R. Machireddy, S. Seshadri, Characterization of biomechanical properties of agar based tissue mimicking phantoms for ultrasound stiffness imaging techniques, J. Mech. Behav. Biomed. Mater. 35 (2014) 132–143, https://doi.org/10.1016/J.JMBBM.2014.03.017.
[36] H. Gojzewski, M. Makowski, A. Hashim, P. Kopcansky, Z. Tomori, M. Timko, Magnetosomes on surface: an imaging study approach, Scanning 34 (2012) 159–169, https://doi.org/10.1002/sca.20292.
[37] R. Prozorov, T. Prozorov, S.K. Mallapragada, B. Narasimhan, T.J. Williams, D.A. Bazylinski, Magnetic irreversibility and the Verwey transition in nanocrystalline bacterial magnetite, Phys. Rev. B 76 (2007), 054406, https://doi.org/10.1103/PhysRevB.76.054406.
[38] E. Alphandéry, Applications of magnetosomes synthesized by magnetotactic bacteria in medicine, Front. Bioeng. Biotechnol. 2 (2014) 5, https://doi.org/10.3389/fbioe.2014.00005.
[39] C. Martinez-Boubeta, K. Simeonidis, A. Makridis, M. Angelakeris, O. Iglesias, P. Guardia, A. Cabot, L. Yedra, S. Estradé, F. Peiró, Z. Saghi, P.A. Midgley, I. Conde-Leborán, D. Serantes, D. Baldomir, Learning from nature to improve the heat generation of Iron-oxide nanoparticles for magnetic hyperthermia applications, Sci. Rep. 3 (2013) 1652, https://doi.org/10.1038/srep01652.
[40] A. Espinosa, R. Di Corato, J. Kolosnjaj-Tabi, P. Flaud, T. Pellegrino, C. Wilhelm, Duality of Iron oxide nanoparticles in cancer therapy: amplification of heating efficiency by magnetic hyperthermia and photothermal bimodal treatment, ACS Nano 10 (2016) 2436–2446, https://doi.org/10.1021/acsnano.5b07249.
[41] K. Kaczmarek, T. Hornowski, I. Antal, M. Timko, A. Józefczak, Magneto-ultrasonic heating with nanoparticles, J. Magn. Magn. Mater. 474 (2019) 400–405, https://doi.org/10.1016/J.JMMM.2018.11.062.